DOTS: Decoupling Operation and Topology in Differentiable Architecture Search

Anonymous authors
Paper under double-blind review

Abstract

Differentiable Architecture Search (DARTS) has attracted extensive attention due to its efficiency in searching for cell structures. However, DARTS mainly focuses on the operation search, leaving the cell topology implicitly depending on the searched operation weights. Hence, a problem is raised: **can cell topology be well represented by the operation weights?** The answer is negative because we observe that the operation weights fail to indicate the performance of cell topology. In this paper, we propose to **D**ecouple the **O**peration and **T**opology **S**earch (DOTS), which decouples the cell topology representation from the operation weights to make an explicit topology search. DOTS is achieved by defining an additional cell topology search space besides the original operation search space. Within the DOTS framework, we propose group annealing operation search and edge annealing topology search to bridge the optimization gap between the searched over-parameterized network and the derived child network. DOTS is efficient and only costs 0.2 and 1 GPU-day to search the state-of-the-art cell architectures on CIFAR and ImageNet, respectively. By further searching for the topology of DARTS' searched cell, we can improve DARTS' performance significantly. The code will be publicly available.

1 Introduction

Neural Architecture Search (NAS) has attracted extensive attention recently for its potential to automatically find the optimal architecture in a large search space. Previous approaches (Zoph et al., 2018; Liu et al., 2018b; Real et al., 2019) based on reinforcement learning and evolutionary learning require a full training process to validate the architecture performance, which consumes hundreds of GPU days to search. To reduce search time, one-shot methods (Pham et al., 2018) exploit the idea of weight sharing, which trains the *supernet* once and derives child architecture performance from the supernet directly. Recent differentiable architecture search (DARTS) (Liu et al., 2019) also exploits the weight sharing idea and further reduces the search cost by unifying the supernet training and optimal child architecture searching.

DARTS represents cell architecture as a directed acyclic graph. Each edge of the graph refers to candidate operations mixed by learnable operation weights, and each graph node denotes a feature map transformed by mixed operations. DARTS has two hard pruning processes to derive the cell architecture from the learned operation weights after searching. The first is operation pruning that only retains the operation with the largest weight for each edge. The second is edge pruning that retains two edges with the largest edge importance for each graph node. The two pruning processes cause inconsistency between search and evaluation because of two problems:

- **Coupling the operation and topology search.** The edge importance of the searched cell is indicated by the largest operation weight of this edge. However, we observe that the operation weight merely indicates the importance of the operation on the specific edge, but not the evidence that the edge should be retained in the searched cell. In other words, the edge importance indicated by operation weights does not correlate with the stand-alone model accuracy, as depicted in Figure 1a.
- **Optimization gap between search and evaluation.** In the search process, DARTS sums the features encoded by different candidate operations. In the evaluation stage, the candidate operations are hard pruned, except the most important one, leading to an optimization

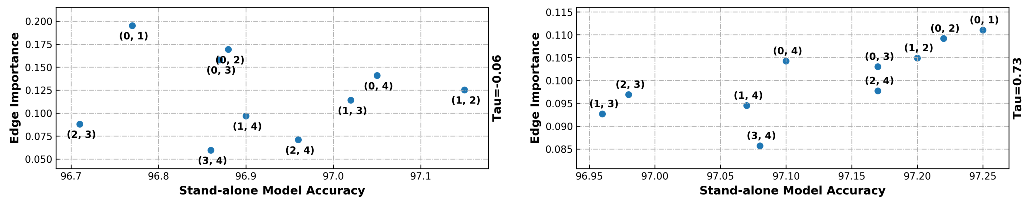

(a) Operation Weight, CIFAR10

(b) Edge Combination Weight, CIFAR10

Figure 1: Correlation between edge importance and stand-alone model accuracy. The edge importance is indicated by (a) operation weight α in DARTS and (b) edge combination weight β in DOTS. We calculate the *Kendall Tau* metric (Kendall, 1938) to measure the ranking correlation between the edge importance and stand-alone model accuracy. The experimental setting can be found in Appendix A.1.

gap between the searched over-parameterized network and the derived child network. The edge pruning encounters a similar optimization gap. Besides, previous works (Chen et al., 2019; Li et al., 2019) show that the network depth gap between search and evaluation is also an optimization gap that causes performance drop.

This paper addresses the first coupling problem via **D**ecoupling **O**peration and **T**opology **S**earch (DOTS). To decouple the edge importance from operation weights, we define a topology search space as the pairwise combinations of edges and make continuous relaxation. The overall search phase is divided into operation search and topology search, in which we update operation weights and edge combination weights, respectively. We address the second problem of the optimization gap by annealing the search process. For operation search, we propose group annealing that divides operation candidates into parameterized and non-parameterized groups. Each group searches and anneals its operation weights to avoid unfair competition (Chu et al., 2019b). Furthermore, we propose edge combination annealing that extends the annealing idea to topology search. As a result, we can further improve DARTS by topology search based on its original searched operations.

We summarize our contributions as follows:

1. Based on the observation that the edge importance indicated by DARTS' operation weights does not correlate with the stand-alone model accuracy, we propose to decouple the operation and topology search (DOTS).
2. We design group annealing operation search and edge annealing topology search within the DOTS framework to bridge the optimization gap.
3. With the reduction of operation candidates, the topology search is efficient. DOTS only costs 0.2 GPU-days to search the state-of-the-art model for CIFAR10/100 (Krizhevsky et al., 2009) and 1 GPU-day for ImageNet (Deng et al., 2009).

1.1 Related Work

Neural Architecture Search (NAS) is an emerging research field for designing neural networks automatically. Previous methods based on reinforcement learning (Zoph & Le, 2017; Zoph et al., 2018) and evolutionary algorithm (Xie & Yuille, 2017; Real et al., 2019) consume large computational overhead. Recent one-shot NAS methods (Brock et al., 2018; Bender et al., 2018; Guo et al., 2019; Chu et al., 2019a) exploit the idea of weight sharing (Pham et al., 2018), which only trains the *supernet* once and thus reduces the search cost. Differentiable NAS (DARTS) (Liu et al., 2019) unifies the supernet training and child architecture searching by continuous relaxation to the architecture search space, making the search more efficient.

Previous works based on DARTS focus on operation search and try to overcome the instability of DARTS. Among them, DARTS+ (Liang et al., 2019) and RobustDARTS (Zela et al., 2020) diagnose DARTS' failure pattern and present an early stop mechanism. P-DARTS (Chen et al., 2019) adds dropout regularization (Srivastava et al., 2014) behind skip-connections and manually restricts the number of skip-connections. FairDARTS (Chu et al., 2019b) argues that DARTS' collapse comes from unfair competition among operations. Recent work (Shu et al., 2020) investigates the cell architecture pattern generated by cell-based NAS and finds that DARTS prefers shallow architectures due to their fast convergence, motivating us to rethink the topology representation in the DARTS framework. Our work improves DARTS by decoupling the topology representation from operation weights and searching for the cell topology explicitly.

P-DARTS (Chen et al., 2019) finds that the depth gap between search and evaluation causes performance drop for searched cells. StackNAS (Li et al., 2019) uses the gradient fusion (Sankararaman et al., 2020) to measure the optimization difficulty between search and evaluation, which provides a theoretical explanation for the depth gap. Besides the depth gap, another optimization gap also causes performance drop. It comes from the gap between the over-parameterized network and the derived child network. ASAP (Noy et al., 2020) and SNAS (Xie et al., 2019) propose operation weight annealing to gradually bridge the optimization gap. However, both methods only target for the operation search and only achieve limited performance. In this work, we propose a stable operation group annealing method and then extend the annealing idea into topology search.

2 Diagnosing the Coupling Problem in DARTS

2.1 Preliminary of Differentiable Architecture Search

We start by reviewing the baseline algorithm DARTS (Liu et al., 2019). DARTS aims at searching for the cell, a repeating building block of the neural network. A cell is represented as a directed cyclic graph with N nodes $\{x_i\}_{i=1}^{N}$, including two input, one output, and several intermediate nodes. Each node denotes a feature map transformed by graph edges. The j-th intermediate node x_j connects to all its predecessors x_i through the edge (i, j). Each edge (i, j) contains candidate operations weighted by the operation weight $\alpha^{(i,j)}$, which can be defined as

$$\bar{o}^{(i,j)}(x) = \sum_{o \in O} \alpha_o^{(i,j)} o^{(i,j)}(x_i), \tag{1}$$

where $o(x) \in \mathcal{O}$ and $\mathcal{O}$ is the operation search space containing eight operations, including *Zero*, *Skip-Connection*, *Avg-Pooling*, *Max-Pooling*, *Sep3x3Conv*, *Sep5x5Conv*, *Dil3x3Conv*, and *Dil5x5Conv*. The weight for each operation is normalized with softmax:

$$\alpha_o^{(i,j)} = \frac{\exp({\alpha'}_o^{(i,j)})}{\sum_{o' \in \mathcal{O}} \exp({\alpha'}_{o'}^{(i,j)})}, \tag{2}$$

where α' is the unnormalized operation weight. The operation weight is updated with the supernet training, gradually focusing on the optimal architecture. Once defined the mixed operation $\bar{o}^{(i,j)}$ for edge (i, j), the intermediate node x_j is computed from all its predecessors x_i:

$$x_j = \sum_{i<j} \bar{o}^{(i,j)}(x_i). \tag{3}$$

After searching, the final architecture is derived from the operation weight α by two hard pruning:

1. Retain the operation with the largest weight and prune other operations for each edge, *i.e.*, $o^{(i,j)} = \arg\max_{o \in \mathcal{O}, o \neq Zero} \alpha_o^{(i,j)}$.
2. Retain two incoming edges with the largest edge importance for each intermediate node and prune other edges. The edge importance is defined as the largest operation weight on each edge (i, j), *i.e.*, $\max_{o \in \mathcal{O}, o \neq Zero} \alpha_o^{(i,j)}$.

The hard pruning causes the optimization gap between the searched over-parameterized network and the derived child network, causing a performance drop of the searched cell (Xie et al., 2019; Noy et al., 2020).

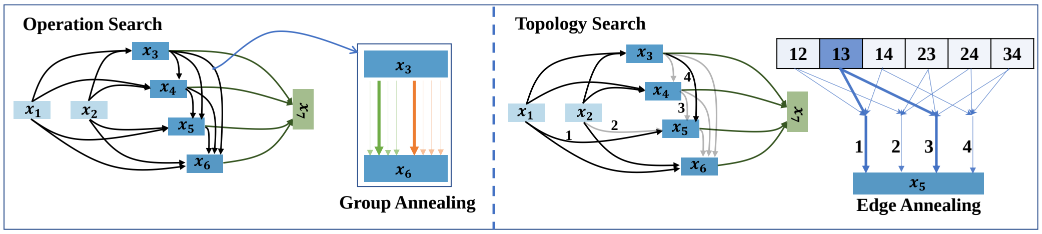

Figure 2: Overall pipeline of the proposed DOTS. The DOTS framework consists of group annealing operation search and edge annealing topology search.

2.1.1 Drawback of Coupling Operation and Topology Search

Previous DARTS-based works search for the cell's operations, while implicitly indicating the edge importance through the largest operation weight. Then, a question is raised: can the operation weight well indicate the edge importance? Following DARTS' policy that retains two edges for each intermediate node, we enumerate all pairwise edge combinations for the intermediate nodes. We calculate the *Kendall Tau* metric (Kendall, 1938) to measure the ranking correlation between the stand-alone model accuracy and edge importance, as depicted in Figure 1. Figure 1a shows that the stand-alone model accuracy has no clear ranking correlation with edge importance indicated by the operation weight. It implies that DARTS' searched cell is sub-optimal because it cannot converge to the best cell topology, which is consistent with the finding that DARTS cannot surpass random search in some cases (Zela et al., 2020). Intuitively, the larger operation weight can only indicate an operation's suitability for a specific edge, but does not mean the edge should be retained in the searched topology. Motivated by this observation, we design edge combination weight to indicate edge importance. Figure 1b demonstrates that the edge combination weight has a better ranking correlation with the stand-alone model accuracy.

3 Methodology

The above analyses expose the drawback of coupling the operation and topology search, *i.e.*, the edge importance indicated by the operation weight does not correlate with the stand-alone model accuracy. In this section, we try to tackle this problem via decoupling operation and topology search, as shown in Figure 2. Within the DOTS framework, we propose group annealing operation search (Section 3.1) and edge annealing topology search (Section 3.2) to bridge the optimization gap.

3.1 Group Annealing Operation Search

With the same graph representation as DARTS, the operation search aims at searching for the best candidate operation for each edge. A straightforward solution is to converge to the best operation directly like DARTS. However, it encounters unfair competition among operations (Chu et al., 2019b). Hence, skip-connections dominate the searched operations, which is sub-optimal for the subsequent topology search. To avoid pruning useful operations too early, we propose the group annealing, which firstly divides operations into two groups based on whether they have learnable parameters and then makes a continuous relaxation in each operation group. With group annealing, we can encourage fair competition within each group and avoid unfair competition between groups.

Formally, the operation search space $\mathcal{O}$ is divided into two sub-search spaces $\mathcal{O}_p$ and $\mathcal{O}_f$ based on whether an operation has learnable parameters or not. In DARTS' search space, $\mathcal{O}_p$ contains *Zero*, *Skip-Connection*, *Avg-Pooling*, and *Max-Pooling*, and $\mathcal{O}_f$ contains *Sep3x3Conv*, *Sep5x5Conv*, *Dil3x3Conv*, and *Dil5x5Conv*. We relax these two sub-search spaces as

$$\alpha_{o_p}^{(i,j)} = \frac{\exp({\alpha'}_{o_p}^{(i,j)}/T)}{\sum_{o'_p \in \mathcal{O}_p} \exp({\alpha'}_{o'_p}^{(i,j)}/T)}, \qquad \alpha_{o_f}^{(i,j)} = \frac{\exp({\alpha'}_{o_f}^{(i,j)}/T)}{\sum_{o'_f \in \mathcal{O}_f} \exp({\alpha'}_{o'_f}^{(i,j)}/T)}, \tag{4}$$

where T is the annealing temperature. $\alpha_{o_p}^{(i,j)}$ and $\alpha_{o_f}^{(i,j)}$ are the normalized operation weights in the groups of $\mathcal{O}_p$ and $\mathcal{O}_f$, respectively.

In Section 2.1, we have reviewed that DARTS has two hard pruning processes after searching, which causes an optimization gap between the searched over-parameterized and derived child networks. To bridge this optimization gap, we anneal the operation weights during searching. When we have $T \to \infty$, the operation weights tend to be uniform. When T gradually anneals to 0, the operation weights tend to be sparse, which is consistent with the hard pruning after searching. We adopt an exponential schedule for annealing:

$$T(t) = T_0\theta^t, \tag{5}$$

where we start with a high initial temperature T_0 that is decayed with the training step t increasing. After searching, the operation with the largest weight is chosen from each group:

$$o_p^{(i,j)} = \arg\max_{o_p \in \mathcal{O}_p} \alpha_{o_p}^{(i,j)}, \qquad o_f^{(i,j)} = \arg\max_{o_f \in \mathcal{O}_f} \alpha_{o_f}^{(i,j)}. \tag{6}$$

After group annealing operation search, the two candidate operations on each edge (i,j) form a new operation search space $\mathcal{O}_n$ for topology search:

$$\mathcal{O}_n = \{o_p^{(i,j)}, o_f^{(i,j)} | 0 < i < j, 2 < j < N\}. \tag{7}$$

Let $\mathcal{L}_{cls}^{train}$ and $\mathcal{L}_{cls}^{val}$ be the Cross-Entropy classification loss on the training and validation sets, respectively, so we can formulate the bi-level optimization with the operation weight $\alpha = \{\alpha_p, \alpha_f\}$ and the network weight w as

$$\begin{aligned} &\min_{\alpha} \;\; \mathcal{L}_{cls}^{val}(w^*(\alpha), \alpha), \\ &\text{s.t. } \; w^*(\alpha) = \arg\min_{w}(\mathcal{L}_{cls}^{train}(w, \alpha)). \end{aligned} \tag{8}$$

We show the results of $\mathcal{O}_n$ searched by the proposed group annealing operation search in Appendix B, and we compare it with DARTS' searched operation candidates in Section 4.3.

3.2 Edge Annealing Topology Search

In Section 2.1.1, we have discussed the drawback of coupling operation and topology search. Hence, we need to decouple the edge importance from operation weights. To achieve this, we define a topology search space and make continuous relaxation to it. Furthermore, we propose edge annealing for topology search to bridge the optimization gap, sharing similar spirits with the group annealing in operation search.

Formally, the incoming edges for each intermediate node x_j connect to all its predecessors. We aim to retain two important edges, *i.e.*, an edge combination, after topology search. Therefore, the topology search space $\mathcal{E}_{x_j}$ for the intermediate node x_j can be defined as all its edge combinations:

$$\mathcal{E}_{x_j} = \{\langle (s,j), (t,j) \rangle \,|0 < s < t < j\}, \tag{9}$$

where x_s, x_t are the predecessors of x_j with the order $s < t$. The topology search space for node x_j contains $C_n^k = \frac{n!}{k!(n-k)!}$ candidate combinations, where we have $k = 2$ and $n = j$. For each node x_j, we relax its topology search space to continuous, which can be defined as

$$\beta_e^{x_j} = \frac{\exp({\beta'}_e^{x_j}/T)}{\sum_{e' \in \mathcal{E}_{x_j}} \exp({\beta'}_{e'}^{x_j}/T)}, \tag{10}$$

where T is the annealing temperature for topology search, $\beta_e^{x_j}$ is the weight for the node x_j and edge combination e. We follow Eq. 1 and Eq. 2 to define the mixed operation $\bar{o}_n$ and operation weight α_{o_n} on the new operation search space $\mathcal{O}_n$ obtained in Eq. 7. The architecture weights in topology search contain the operation weight $\alpha = \{\alpha_{o_n}^{(i,j)}\}$ and edge combination weight $\beta = \{\beta_e^{x_j}\}$. The feature on the node x_j is the weighted sum of all incoming edges:

$$x_j = \sum_{i<j} \gamma^{(i,j)} \cdot \bar{o}_n^{(i,j)}(x_i), \tag{11}$$

where $\gamma^{(i,j)} = \sum_{c \in \mathcal{E}_{x_j}, (i,j) \in c} \beta_c^{x_j}$ aggregates the weight for edge (i,j) from all its combinations, as shown in Figure 2. To bridge the optimization gap in topology search, we anneal the operation

Table 1: Comparison with state-of-the-art NAS algorithms on CIFAR10.

Architecture	Test Err. (%)	Params (M)	Search Cost (GPU Days)	Search Method
DenseNet-BC (Huang et al., 2017)	3.46	25.6	N/A	N/A
NASNet-A (Zoph et al., 2018)	2.65	3.3	1800	RL
ENAS (Pham et al., 2018)	2.89	4.6	0.5	RL
NAONet-WS (Luo et al., 2018)	3.53	3.1	0.4	NAO
AmoebaNet-B (Real et al., 2019)	2.55± 0.05	2.8	3150	EA
Hireachical Evolution (Liu et al., 2018b)	3.75± 0.12	15.7	300	EA
PNAS (Liu et al., 2018a)	3.41± 0.09	3.2	225	SMBO
DARTS (Liu et al., 2019)	3.00	3.3	0.4	GD
SNAS (Xie et al., 2019)	2.85	2.8	1.5	GD
GDAS (Dong & Yang, 2019)	2.93	2.5	0.2	GD
P-DARTS (Chen et al., 2019)	2.50	3.4	0.3	GD
FairDARTS (Chu et al., 2019b)	2.54	2.8	0.4	GD
PC-DARTS (Xu et al., 2020)	2.57 ± 0.07	3.6	0.1	GD
DropNAS (Hong et al., 2020)	2.58 ± 0.14	4.1	0.6	GD
MergeNAS (Wang et al., 2020)	2.73 ± 0.02	2.9	0.2	GD
ASAP (Noy et al., 2020)	2.68 ± 0.11	2.5	0.2	GD
SDARTS-ADV (Chen & Hsieh, 2020)	2.61 ± 0.02	3.3	1.3	GD
DARTS- (Chu et al., 2020)	2.59 ± 0.08	3.5	0.4	GD
DOTS	**2.45 ± 0.04**	4.2	0.2	GD

weight α and edge combination weight β with the exponential schedule defined in Eq. 5. We mainly focus on the topology search in this phase, so we adopt a low initial temperature T_0 for annealing operation weight α_{o_n}, making the operation on each edge almost fixed in the first few epochs.

DARTS uses bi-level optimization to avoid overfitting (Liu et al., 2019). However, Li et al. (2019) shows that one-level optimization is more stable and accurate than bi-level optimization. The topology search is performed in a reduced operation search space, which eliminates the risk of overfitting. Therefore, we use one-level optimization for updating both the network weight w and the architecture weight $\phi = \{\alpha, \beta\}$, which can be formulated as

$$\begin{aligned} w_t &= w_{t-1} - \eta_t \partial_w L_{train}(w_{t-1}, \phi_{t-1}), \\ \phi_t &= \phi_{t-1} - \delta_t \partial_w L_{train}(w_{t-1}, \phi_{t-1}), \end{aligned} \tag{12}$$

where η_t and δ_t are the learning rates of the network weight and architecture weight, respectively.

4 Experiment

4.1 Evaluation on the CIFAR10 Dataset

Search Settings. The whole search process on CIFAR10 (Krizhevsky et al., 2009) takes 60 epochs, *i.e.*, 25 epochs for the operation search stage and 35 for the topology search stage. We pretrain network weights in the first 15 epochs of both stages by only updating network weights. The network is composed of 8 cells for operation search and 17 cells for topology search. The initial temperature T_0 is 10 for both stages, while the minimum temperature for operation search and topology search is 0.2 and 0.02, respectively. The search process costs 4.9 hours on one NVIDIA Quadro RTX 8000 GPU. More detailed search settings can be found in Appendix A.2.

Evaluation Settings. The evaluation settings follow DARTS (Liu et al., 2019). The network is composed of 20 cells (18 normal cells and 2 reduction cells) and the initial number of channels is 36. We train the network from scratch for 600 epochs with a batch size of 96. The network is optimized via the SGD optimizer with an initial learning rate of 0.025 (cosine annealing to 0), momentum of 0.9, weight decay of 3e-4, and gradient clipping at 5. Cutout and drop path with a rate of 0.2 are used for preventing from overfitting. We follow DARTS to run the evaluation five times and report the average results of the searched cell.

Table 2: Comparison with state-of-the-art NAS algorithms on ImageNet. CIFAR10/ImageNet means the cell architecture is searched on CIFAR10 or ImageNet.

Architecture	Test Err. (%)		Params (M)	Multi-Add (M)	Search Cost (GPU-days)	Search Method
	top-1	top-5				
Inception-v1 (Szegedy et al., 2015)	30.2	10.1	6.6	1448	N/A	N/A
MobileNet (Howard et al., 2017)	29.4	10.5	4.2	569	N/A	N/A
ShuffleNet 2× (v1) (Zhang et al., 2018)	26.4	10.2	5.4	524	N/A	N/A
ShuffleNet 2× (v2) (Ma et al., 2018)	25.1	7.6	7.4	591	N/A	N/A
NASNet-A (Zoph et al., 2018)	26.0	8.4	5.3	564	1800	RL
AmoebaNet-C (Real et al., 2019)	24.3	7.6	6.4	570	3150	EA
PNAS (Liu et al., 2018a)	25.8	8.1	5.1	588	225	SMBO
MnasNet-92 (Tan et al., 2019)	25.2	8.0	4.4	388	1667	RL
DARTS (2nd order) (CIFAR10) (Liu et al., 2019)	26.7	8.7	4.7	574	4.0	GD
SNAS (CIFAR10) (Xie et al., 2019)	27.3	9.2	4.3	522	1.5	GD
P-DARTS (CIFAR10) (Chen et al., 2019)	24.4	7.4	4.9	557	0.3	GD
GDAS (Dong & Yang, 2019)	26.0	8.5	5.3	581	0.2	GD
FairDARTS (CIFAR10) (Chu et al., 2019b)	24.9	7.5	4.8	541	0.4	GD
PC-DARTS (CIFAR10) (Xu et al., 2020)	25.1	7.8	5.3	586	0.1	GD
SDARTS-ADV (CIFAR10) (Chen & Hsieh, 2020)	25.2	7.8	5.4	594	1.3	GD
DOTS (CIFAR10)	24.4	7.5	5.0	557	0.2	GD
ProxylessNAS (ImageNet) (Cai et al., 2019)	24.9	7.5	7.1	465	8.3	GD
FairDARTS (ImageNet) (Chu et al., 2019b)	24.4	7.4	4.3	440	3	GD
PC-DARTS (ImageNet) (Xu et al., 2020)	24.2	7.3	5.3	597	3.8	GD
DOTS (ImageNet)	**24.0**	**7.2**	5.3	596	1.0	GD

Main Results. The evaluation results on CIFAR10 are shown in Table 1 (The evaluation results on CIFAR100 can be found in Appendix C). The DOTS' search cost of 0.2 GPU-Days is more efficient than that of P-DARTS, where both methods search for a deeper network to bridge the depth gap. ASAP (Noy et al., 2020) proposes the operation annealing and pruning, but it suffers from unfair operation competition so that skip-connections dominate the searched cell. We propose the group annealing operation search and extend the annealing idea to topology search, decreasing ASAP top-1 error by 0.23%. The searched cells are shown in Figure 4 in the appendix.

4.2 Evaluation on the ImageNet Dataset

Search Settings. We randomly sample 10% and 2.5% images from ImageNet (Deng et al., 2009) to build the training and validation sets, following PC-DARTS (Xu et al., 2020). For the bi-level optimization, the training set and the validation set are used to update network weights and architecture weights, respectively. For the one-level optimization, both sets are used to update network weights and architecture weights simultaneously. The whole search process takes 60 epochs, equally divided into the operation search and topology search stages, where the first 15 epochs of both stages are used to pretrain the network weights. The network is composed of 8 cells for operation search and 14 cells for topology search. The initial temperature T_0 is 10 for both stages, while the minimum temperature for operation search and topology search is 0.1 and 0.01, respectively. The search process costs 11.6 hours on two NVIDIA Quadro RTX 8000 GPUs. More detailed search settings can be found in Appendix A.2.

Evaluation Settings. We use the mobile setting, where the input image size is set to 224×224, and the number of multiply-add operations is restricted to be fewer than 600M. The evaluation settings follow PC-DARTS (Chen et al., 2019). The network consists of 14 cells (12 normal cells and 2 reduction cells) with an initial number of channels of 46. We train the network from scratch for 250 epochs with a batch size of 1024. The SGD optimizer with an initial learning rate of 0.5 (warm up in the first 5 epochs and cosine annealing to 0), momentum of 0.9, and weight decay of $3e$-5 is used. Additional enhancements follow P-DARTS and PC-DARTS, including label smoothing and an auxiliary loss tower. We evaluate both the cell directly searched on ImageNet and the cell transferred from CIFAR10.

Main Results. The evaluation results are summarized in Table 2. Most gradient-based methods search on a proxy dataset, *e.g.*, CIFAR, and transfer the searched cell to ImageNet because their search cost on ImageNet is prohibitive. In contrast, DOTS can search on ImageNet proxylessly, and requires the least search cost (1 GPU-Day). DOTS decreases the top-1 error of PC-DARTS by 0.2. The searched cells are shown in Figure 6 in the appendix.

Table 3: Ablation study for group annealing and edge annealing.

Group Annealing	Edge Annealing	CIFAR10 Test Err.
✗	✗	2.76±0.09
✓	✗	2.70±0.11
✗	✓	2.57±0.06
✓	✓	**2.45±0.04**

Table 4: Influence of one-level (OL) and bi-level (BL) optimization for different stages.

Operation Search	Topology Search	CIFAR10 Test Err.
OL	OL	2.54 ±0.06
OL	BL	2.59±0.12
BL	OL	**2.45±0.04**
BL	BL	2.66±0.07

Table 5: Improving DARTS' operation search by topology search.

Architecture	CIFAR10 Test Err.
DARTS	2.96±0.12
DARTS+EATS	2.60±0.09
DOTS (GAOS+EATS)	**2.45±0.04**

Table 6: Influence of the number of the searched cell in topology search.

Number of cells	CIFAR10 Test Err.	Search Cost (GPU-days)
8	2.62 ±0.06	**0.14**
14	2.51 ±0.03	0.18
17	**2.45 ±0.04**	0.20

4.3 Ablation Study

Influence of Annealing. We evaluate the improvement brought by the proposed annealing technique, *i.e.*, group annealing and edge annealing. From results in Table 3, the reduction on top-1 error brought by edge annealing is 0.25% (2.70% to 2.45%), and that brought by group annealing is 0.12% (2.57% to 2.45%). The improvement of group annealing is smaller than edge annealing. This is because the former divides the operations into parameterized and non-parameterized groups, which ensures that essential candidate operations within each group are retained.

Influence of the Optimization Level. DARTS (Liu et al., 2019) finds that architecture weights are easy to overfit with one-level optimization, but one-level optimization is found to be stable in StacNas (Li et al., 2019). In DOTS, the topology search is performed in a reduced search space, which is less risk of overfitting. As the results in Table 4, one-level optimization has better performance (2.45% *vs*. 2.66%) than bi-level optimization for searching topology.

Improving DARTS' Operation Search. Section 2.1.1 discusses that DARTS can not converge to the optimal topology because it couples the operation and topology search. Treated DARTS as an operation search method, we show in Table 5 that DARTS' results can be improved (2.96% *vs*. 2.60%) by incorporating the proposed edge annealing topology search (**EATS**). Meantime, replacing the candidate operation searched by DARTS with that searched by the proposed group annealing operation search (GAOS) further improves the performance (2.60% *vs*. 2.45%).

Bridging the Depth Gap. With the reduction of candidate operations in topology search, we can stack more layers to bridge the depth gap for searching better topology with slight memory cost. Table 6 shows that the performance improves with the reduction of the depth gap. In our work, we use 17 layers for searching topology in CIFAR without further clarification.

5 Conclusion

We have introduced DOTS that decouples operation search and topology search in differentiable neural architecture search, based on the observation that the edge importance indicated by operation weights does not correlate with the stand-alone model accuracy. Specifically, we define the cell topology search space and make it continuous by introducing edge combination weights. The edge importance indicated by edge combination weights strongly correlates with stand-alone model accuracy. Within the DOTS framework, we propose group annealing and edge combination annealing to bridge the optimization gap. Thanks to the reduced candidate operations in topology search, we can stack more cells to bridge the depth gap with slight memory cost. DOTS costs 0.2 and 1 GPU-days to search the state-of-the-art architectures on CIFAR and ImageNet, respectively. We improve DARTS' searched cell by further searching its topology, showing the effectiveness of DOTS.

REFERENCES

Gabriel Bender, Pieter-Jan Kindermans, Barret Zoph, Vijay Vasudevan, and Quoc V. Le. Understanding and simplifying one-shot architecture search. In *ICML*, pp. 549–558, 2018.

Andrew Brock, Theo Lim, J.M. Ritchie, and Nick Weston. SMASH: One-shot model architecture search through hypernetworks. In *ICLR*, 2018.

Han Cai, Ligeng Zhu, and Song Han. ProxylessNAS: Dsearchirect neural architecture search on target task and hardware. In *ICLR*, 2019.

Xiangning Chen and Cho-Jui Hsieh. Stabilizing differentiable architecture search via perturbation-based regularization. In *ICML*, 2020.

Xin Chen, Lingxi Xie, Jun Wu, and Qi Tian. Progressive differentiable architecture search: Bridging the depth gap between search and evaluation. In *IEEE ICCV*, pp. 1294–1303, 2019.

Xiangxiang Chu, Bo Zhang, Ruijun Xu, and Jixiang Li. Fairnas: Rethinking evaluation fairness of weight sharing neural architecture search. *arXiv preprint arXiv:1907.01845*, 2019a.

Xiangxiang Chu, Tianbao Zhou, Bo Zhang, and Jixiang Li. Fair darts: Eliminating unfair advantages in differentiable architecture search. *arXiv preprint arXiv:1911.12126*, 2019b.

Xiangxiang Chu, Xiaoxing Wang, Bo Zhang, Shun Lu, Xiaolin Wei, and Junchi Yan. Darts-: Robustly stepping out of performance collapse without indicators. *arXiv preprint arXiv:2009.01027*, 2020.

Jia Deng, Wei Dong, Richard Socher, Li-Jia Li, Kai Li, and Li Fei-Fei. Imagenet: A large-scale hierarchical image database. In *IEEE CVPR*, pp. 248–255, 2009.

Xuanyi Dong and Yi Yang. Searching for a robust neural architecture in four gpu hours. In *IEEE CVPR*, pp. 1761–1770, 2019.

Zichao Guo, Xiangyu Zhang, Haoyuan Mu, Wen Heng, Zechun Liu, Yichen Wei, and Jian Sun. Single path one-shot neural architecture search with uniform sampling. *arXiv preprint arXiv:1904.00420*, 2019.

Kaiming He, Xiangyu Zhang, Shaoqing Ren, and Jian Sun. Deep residual learning for image recognition. In *IEEE CVPR*, pp. 770–778, 2016.

Weijun Hong, Guilin Li, Weinan Zhang, Ruiming Tang, Yunhe Wang, Zhenguo Li, and Yong Yu. DropNAS: Grouped operation dropout for differentiable architecture search. In *IJCAI*, pp. 2326–2332, 2020.

Andrew G Howard, Menglong Zhu, Bo Chen, Dmitry Kalenichenko, Weijun Wang, Tobias Weyand, Marco Andreetto, and Hartwig Adam. Mobilenets: Efficient convolutional neural networks for mobile vision applications. *arXiv preprint arXiv:1704.04861*, 2017.

Gao Huang, Zhuang Liu, Laurens Van Der Maaten, and Kilian Q Weinberger. Densely connected convolutional networks. In *IEEE CVPR*, pp. 4700–4708, 2017.

Maurice G Kendall. A new measure of rank correlation. *Biometrika*, 30(1/2):81–93, 1938.

Alex Krizhevsky et al. Learning multiple layers of features from tiny images. 2009.

Guilin Li, Xing Zhang, Zitong Wang, Zhenguo Li, and Tong Zhang. StacNAS: Towards stable and consistent optimization for differentiable neural architecture search. *arXiv preprint arXiv:1909.11926*, 2019.

Hanwen Liang, Shifeng Zhang, Jiacheng Sun, Xingqiu He, Weiran Huang, Kechen Zhuang, and Zhenguo Li. Darts+: Improved differentiable architecture search with early stopping. *arXiv preprint arXiv:1909.06035*, 2019.

Chenxi Liu, Barret Zoph, Maxim Neumann, Jonathon Shlens, Wei Hua, Li-Jia Li, Li Fei-Fei, Alan Yuille, Jonathan Huang, and Kevin Murphy. Progressive neural architecture search. In *ECCV*, pp. 19–34, 2018a.

Hanxiao Liu, Karen Simonyan, Oriol Vinyals, Chrisantha Fernando, and Koray Kavukcuoglu. Hierarchical representations for efficient architecture search. In *ICLR*, 2018b.

Hanxiao Liu, Karen Simonyan, and Yiming Yang. DARTS: Differentiable architecture search. In *ICLR*, 2019.

Renqian Luo, Fei Tian, Tao Qin, Enhong Chen, and Tie-Yan Liu. Neural architecture optimization. In *NIPS*, pp. 7816–7827, 2018.

Ningning Ma, Xiangyu Zhang, Hai-Tao Zheng, and Jian Sun. Shufflenet v2: Practical guidelines for efficient cnn architecture design. In *ECCV*, pp. 116–131, 2018.

Asaf Noy, Niv Nayman, Tal Ridnik, Nadav Zamir, Sivan Doveh, Itamar Friedman, Raja Giryes, and Lihi Zelnik. Asap: Architecture search, anneal and prune. In *AISTATS*, pp. 493–503, 2020.

Hieu Pham, Melody Y. Guan, Barret Zoph, Quoc V. Le, and Jeff Dean. Efficient neural architecture search via parameter sharing. In *ICML*, 2018.

Esteban Real, Alok Aggarwal, Yanping Huang, and Quoc V Le. Regularized evolution for image classifier architecture search. In *AAAI*, volume 33, pp. 4780–4789, 2019.

Karthik A Sankararaman, Soham De, Zheng Xu, W Ronny Huang, and Tom Goldstein. The impact of neural network overparameterization on gradient confusion and stochastic gradient descent. In *ICML*, 2020.

Yao Shu, Wei Wang, and Shaofeng Cai. Understanding architectures learnt by cell-based neural architecture search. In *ICLR*, 2020.

Nitish Srivastava, Geoffrey Hinton, Alex Krizhevsky, Ilya Sutskever, and Ruslan Salakhutdinov. Dropout: a simple way to prevent neural networks from overfitting. *JMLR*, 15(1):1929–1958, 2014.

Christian Szegedy, Wei Liu, Yangqing Jia, Pierre Sermanet, Scott Reed, Dragomir Anguelov, Dumitru Erhan, Vincent Vanhoucke, and Andrew Rabinovich. Going deeper with convolutions. In *IEEE CVPR*, pp. 1–9, 2015.

Mingxing Tan, Bo Chen, Ruoming Pang, Vijay Vasudevan, Mark Sandler, Andrew Howard, and Quoc V Le. Mnasnet: Platform-aware neural architecture search for mobile. In *IEEE CVPR*, pp. 2820–2828, 2019.

Xiaoxing Wang, Chao Xue, Junchi Yan, Xiaokang Yang, Yonggang Hu, and Kewei Sun. MergeNAS: Merge operations into one for differentiable architecture search. In *IJCAI*, pp. 3065–3072, 2020.

Lingxi Xie and Alan Yuille. Genetic cnn. In *IEEE CVPR*, pp. 1379–1388, 2017.

Sirui Xie, Hehui Zheng, Chunxiao Liu, and Liang Lin. SNAS: stochastic neural architecture search. In *ICLR*, 2019.

Yuhui Xu, Lingxi Xie, Xiaopeng Zhang, Xin Chen, Guo-Jun Qi, Qi Tian, and Hongkai Xiong. PC-DARTS: Partial channel connections for memory-efficient architecture search. In *ICLR*, 2020.

Arber Zela, Thomas Elsken, Tonmoy Saikia, Yassine Marrakchi, Thomas Brox, and Frank Hutter. Understanding and robustifying differentiable architecture search. In *ICLR*, 2020.

Xiangyu Zhang, Xinyu Zhou, Mengxiao Lin, and Jian Sun. Shufflenet: An extremely efficient convolutional neural network for mobile devices. In *IEEE CVPR*, pp. 6848–6856, 2018.

Barret Zoph and Quoc V Le. Neural architecture search with reinforcement learning. In *ICLR*, 2017.

Barret Zoph, Vijay Vasudevan, Jonathon Shlens, and Quoc V Le. Learning transferable architectures for scalable image recognition. In *IEEE CVPR*, pp. 8697–8710, 2018.

A Detailed Experimental Settings

A.1 Correlation between Edge Importance and Model Accuracy

The following is the detailed settings for calculating the correlation between edge importance and model accuracy in Figure 1. We use the official public code of DARTS to search on CIFAR10. After searching, we enumerate all pairwise combinations of 5 edges of the last intermediate node, resulting in total 10 edge combinations. For DARTS, edge importance is indicated by the largest operation weight (excluding the *Zero* operation) on this edge. We sum its two edge importance as the importance of an edge combination. In contrast, the edge combination weight of DOTS can directly represent the importance of an edge combination. The stand-alone model is trained with the same settings in Section A.2, except that we reduce the number of training epochs to 300. The results are depicted in Figure 1.

A.2 Detailed Search Settings for Benchmarking

CIFAR. The whole search process takes 60 epochs, *i.e.*, 25 epochs for the operation search stage and 35 epochs for the topology search stage. We pretrain the first 15 epochs of both two stages by only updating network weights. The SGD optimizer is adopted to optimize the network weight w with an initial learning rate of 0.025 (cosine decaying to 0.001 in 60 epochs), weight decay of $3e$-4, and momentum of 0.9. For architecture weights α and β, we use the Adam optimizer with a constant learning weight of $1e$-4 and weight decay of $1e$-3 for both stages. We set $T_0 = 10$ and $\theta = 0.65$ in Eq. 5 for annealing operation weights, while we set $T_0 = 10$ and $\theta = 0.72$ for annealing edge combination weights. The temperature ends at 0.2 and 0.02 for operation search and topology search, respectively.

ImageNet. The search process of ImageNet takes 60 epochs, where both operation search and topology search stages take 30 epochs separately. Both stages pretrain for 15 epochs. The SGD optimizer is used to optimize the network weight w with an initial learning rate of 0.5 (cosine decaying to 0 in 60 epochs), weight decay of $3e$-4, and momentum of 0.9. For the architecture parameters α, we use the Adam optimizer with a constant learning weight of $6e$-3 and weight decay of $1e$-3 for both stages. We set $T_0 = 10$ and $\theta = 0.75$ in Eq. 5 for annealing operation weights, while we set $T_0 = 10$ and $\theta = 0.64$ for annealing edge combination weights. The temperature ends at 0.1 and 0.01 for operation search and topology search, respectively.

B Discussion about the differences between DARTS and DOTS

We analyze the five edges connected to the last intermediate node. As depicted in Figure 3a, the operation weights are affected by the *Zero* operation in DARTS. The weight of the *Zero* operation ends at 0.4 on the shallow edge $(0, 5)$, while it increases to 0.9 on the deepest edge $(4, 5)$. With the increasing weight of the *Zero* operation, the weights of other operations on five edges are all decreasing. Since the operation weights on shallow edges decrease more slowly, the operation weights on shallow edges are larger than that on deep edges. Based on DARTS' policy that edge importance is the largest operation weight (except the *Zero* operation), the two shallowest edges are always retained. By decoupling operation search and topology search, the instability of operation search has no impact on choosing the optimal edges. As the result in Section 4.3, we do not change DARTS' searched operations but re-search its topology, decreasing DARTS' top-1 error by 0.36%.

Since DARTS' operation search is not stable, we aim to design a stable operation search method, *i.e.*, group annealing operation search. As depicted in Figure 3b, we divide the candidate operations into two groups. The *Zero* operation competes with other non-parameterized operations and has no clear advantage, except on the deepest edge. Whatever the non-parameterized operation weights evolve, it will not affect the parameterized operation weights. In a word, we encourage fair competition within each group and avoid unfair competition between groups, making operation search more stable. The candidate operations searched by group annealing operation search are listed in Table 7, Table 8, and Table 9. By replacing DARTS' operation search with group annealing operation search, we further decrease the top-1 error by 0.15%.

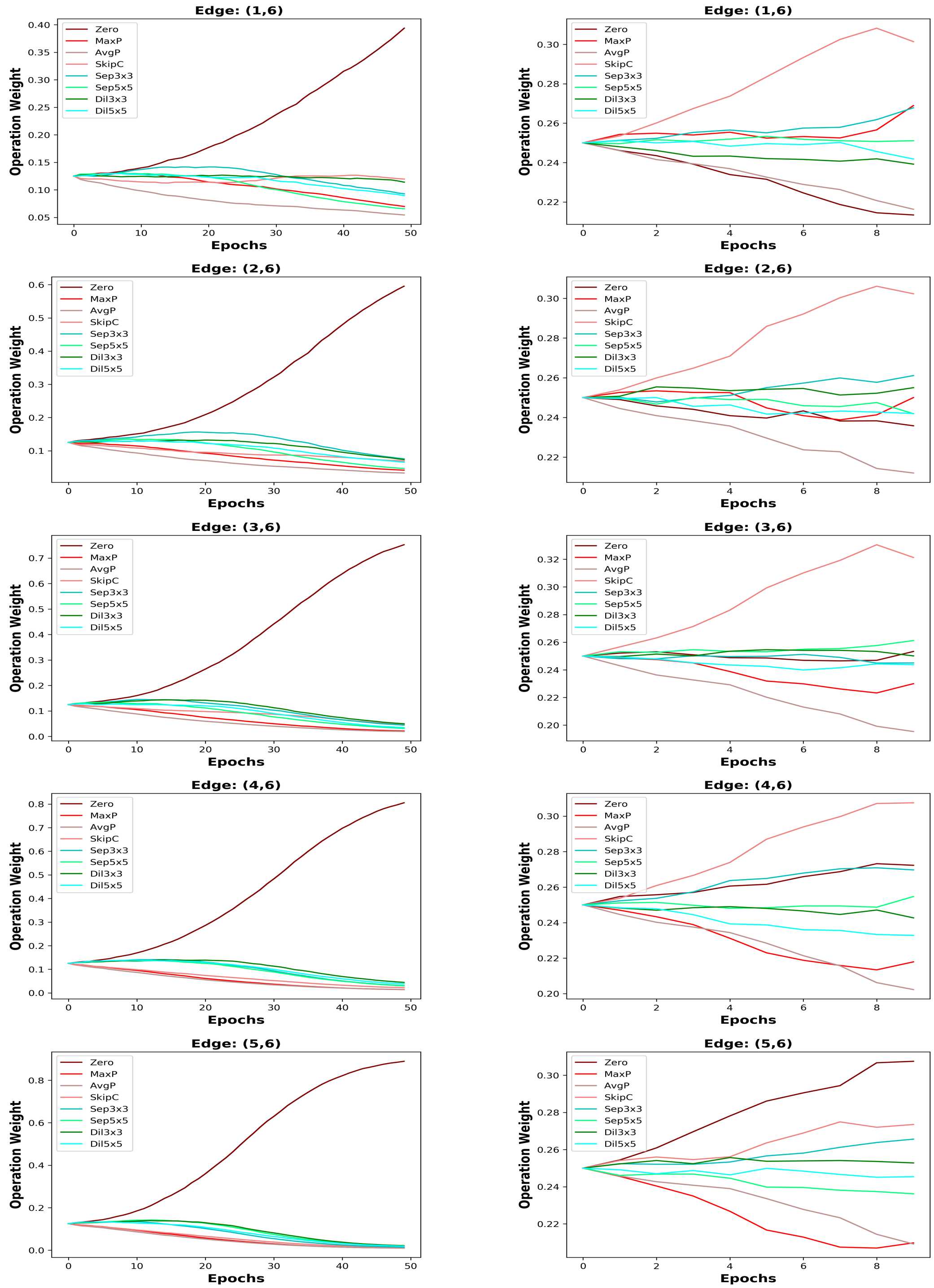

(a) DARTS (b) DOTS

Figure 3: Operation weight evolution during training in DARTS and DOTS. For DOTS, we plot the operation weights without annealing.

Table 7: The operations retained for each group after operation search on CIFAR10.

EdgeID	1	2	3	4	5	6	7
OP Group 1	SkipC	SkipC	SkipC	SkipC	SkipC	SkipC	SkipC
OP Group 2	Sep3x3	Sep3x3	Sep3x3	Sep3x3	Sep3x3	Dil3x3	Sep3x3
EdgeID	8	9	10	11	12	13	14
OP Group 1	SkipC	Zero	SkipC	SkipC	SkipC	SkipC	Zero
OP Group 2	Sep5x5	Dil5x5	Sep3x3	Sep3x3	Sep5x5	Sep3x3	Sep3x3

(a) Normal Cell

EdgeID	1	2	3	4	5	6	7
OP Group 1	AvgP	Zero	AvgP	AvgP	SkipC	AvgP	AvgP
OP Group 2	Dil5x5	Dil3x3	Sep5x5	Dil3x3	Dil5x5	Dil3x3	Dil5x5
EdgeID	8	9	10	11	12	13	14
OP Group 1	SkipC	Zero	AvgP	AvgP	SkipC	SkipC	Zero
OP Group 2	Sep5x5	Sep3x3	Dil3x3	Sep3x3	Dil5x5	Dil5x5	Sep5x5

(b) Reduction Cell

Table 8: The operations retained for each group after operation search on CIFAR100.

EdgeID	1	2	3	4	5	6	7
OP Group 1	SkipC	SkipC	SkipC	SkipC	SkipC	SkipC	SkipC
OP Group 2	Sep3x3	Sep3x3	Sep3x3	Sep3x3	Dil5x5	Sep5x5	Sep3x3
EdgeID	8	9	10	11	12	13	14
OP Group 1	SkipC	Zero	SkipC	SkipC	SkipC	SkipC	Zero
OP Group 2	Sep5x5	Sep3x3	Sep5x5	Dil5x5	Sep3x3	Dil3x3	Dil3x3

(a) Normal Cell

EdgeID	1	2	3	4	5	6	7
OP Group 1	SkipC	Zero	AvgP	MaxP	SkipC	AvgP	MaxP
OP Group 2	Sep3x3	Sep3x3	Sep3x3	Dil5x5	Dil5x5	Dil5x5	Sep3x3
EdgeID	8	9	10	11	12	13	14
OP Group 1	SkipC	Zero	AvgP	MaxP	SkipC	SkipC	Zero
OP Group 2	Dil5x5	Dil5x5	Sep3x3	Sep3x3	Dil5x5	Dil5x5	Dil5x5

(b) Reduction Cell

Table 9: The operations retained for each group after operation search on ImageNet.

EdgeID	1	2	3	4	5	6	7
OP Group 1	SkipC	SkipC	SkipC	SkipC	Zero	Zero	SkipC
OP Group 2	Dil5x5	Dil3x3	Sep3x3	Sep3x3	Sep3x3	Sep3x3	Sep3x3
EdgeID	8	9	10	11	12	13	14
OP Group 1	SkipC	Zero	Zero	SkipC	Zero	Zero	Zero
OP Group 2	Sep3x3	Sep3x3	Sep3x3	Sep5x5	Sep3x3	Dil5x5	Sep3x3

(a) Normal Cell

EdgeID	1	2	3	4	5	6	7
OP Group 1	Zero	SkipC	Zero	SkipC	Zero	MaxP	AvgP
OP Group 2	Sep5x5	Sep3x3	Sep3x3	Sep5x5	Dil5x5	Sep3x3	Sep5x5
EdgeID	8	9	10	11	12	13	14
OP Group 1	Zero	Zero	MaxP	MaxP	SkipC	Zero	Zero
OP Group 2	Sep5x5	Dil5x5	Sep3x3	Dil3x3	Sep3x3	Sep3x3	Sep3x3

(b) Reduction Cell

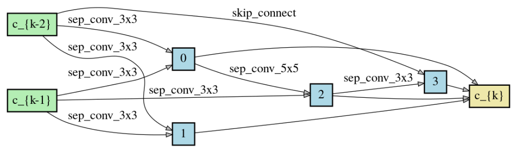

(a) Normal Cell (b) Reduction Cell

Figure 4: Normal cell and reduction cell found by DOTS on CIFAR10.

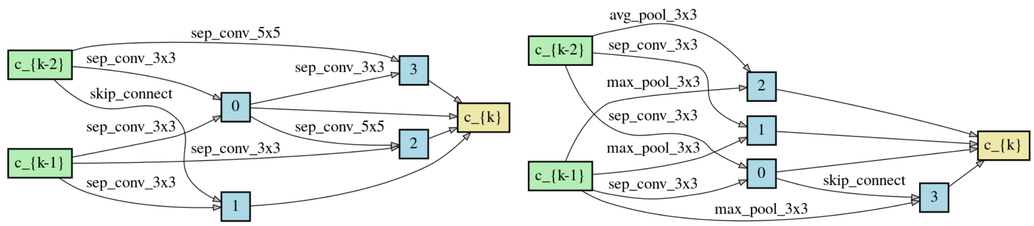

(a) Normal Cell (b) Reduction Cell

Figure 5: Normal cell and reduction cell found by DOTS on CIFAR100.

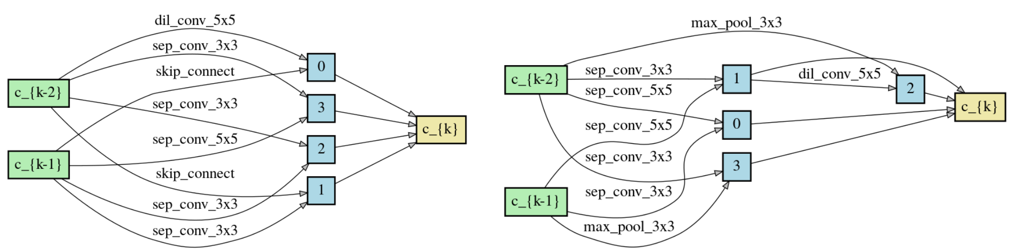

(a) Normal Cell (b) Reduction Cell

Figure 6: Normal cell and reduction cell found by DOTS on ImageNet.

Table 10: Comparison with state-of-the-art NAS algorithms on CIFAR100. † marks the results reported by Chu et al. (2020), and ‡ marks the results taken from the original papers.

Architecture	**Test Err. (%)**	**Params (M)**	**Search Cost (GPU Days)**	**Search Method**
ResNet (He et al., 2016)	22.10†	1.7	N/A	N/A
DenseNet-BC (Huang et al., 2017)	17.18†	25.6	N/A	N/A
AmoebaNet (Real et al., 2019)	18.93†	3.1	3150	EA
PNAS (Liu et al., 2018a)	19.53†	3.2	150	SMBO
ENAS (Pham et al., 2018)	19.43†	4.6	0.45	RL
DARTS (2nd) (Liu et al., 2019)	17.54†	3.4	1	GD
GDAS (Dong & Yang, 2019)	18.38†	3.4	0.2	GD
P-DARTS (Chen et al., 2019)	17.49†	3.6	0.3	GD
DropNAS (Hong et al., 2020)	16.39‡	4.4	0.7	GD
DARTS- (Chu et al., 2020)	17.16‡	3.4	0.4	GD
DOTS	**15.75**	4.2	0.2	GD

C ADDITIONAL BENCHMARKING RESULTS

We benchmark DOTS on CIFAR100 in Table 10. The search setting and the evaluation setting is the same as that on CIFAR10. DOTS decreases the top-1 error of DropNAS by 0.64% and reduces the search cost by 0.5 GPU-Days. We visualize the searched cells in Figure 4, Figure 5, and Figure 6.